Emerging Compressed States of a Spiral Electron Stream in a System with Deceleration

E. N. Egorov*, A. A. Koronovskii, S. A. Kurkin, and A. E. Hramov

Saratov State University, Saratov, 410026 Russia
Saratov State Technical University, Saratov, 410054 Russia
*e-mail: evgeniy.n.egorov@gmail.com
Revised manuscript received March 1, 2013

Abstract—The emergence of a compressed state in an intense electron stream with additional deceleration in a virtual cathode formation mode is considered. The numerical-modeling results of compressed state formation are presented. It is shown that longitudinal oscillations of the density of the spatial charge of a beam may be observable in a system with deceleration in a compressed state.

DOI: 10.1134/S1063785013100039

At present, studies on the formation and nonlinear dynamics of a virtual cathode (VC) in intense electron streams (see, for example, overviews [1–3] and references therein) are of great interest. This is because of the fundamental importance of research into the complex behavior of distributed beam–plasma and electron–wave systems, as well as by their applied relevance for the development of powerful sources of electromagnetic VC radiation, vircators [4].

A promising and important research area here is the study of beam compressed states (BCSs) [3, 5–7], which are characterized by a high density and a low rate of stream electrons in a certain area of the interaction space. To establish BCSs, a composite drift space of tubes of different radii is used, so that, in the first tube with a smaller drift radius, the beam current is lower than the critical current of VC formation and, in the other tube with a larger radius, it is higher. The whole system is placed in a strong longitudinal magnetic field. A BCS is formed in the first area, where the beam current is lower than the limit vacuum current [3, 6], by creating a stationary electron-reflecting VC in the second drift tube with the larger radius. The BCS area is, in fact, a VC distributed in the drift space and characterized by its complex dynamics of stream particles, as well as by various scenarios of its implementation [3, 8]. In [9], the authors substantiated the BCS use for the collective acceleration of ions.

Note that an extended region of the interaction space is necessary for BCS formation, where the beam current is lower than the critical value so that a VC is formed at the output from this instrument section. This can be achieved by a jump in the radius of the drift channel [3], as well as by additional beam deceleration. Previously, we proposed and implemented a modification of the VC generator in which a VC is formed in an intense (with a high perveance) electron stream by additional electron deceleration [10, 11]. Owing to additional electron deceleration, this instrument can reduce the starter current necessary for the formation of a nonstationary oscillating VC. Due to the similarity of VC formation processes in a system with and without deceleration, it is expected that a system with deceleration can establish a BCS. The purpose of this paper is to investigate the possibility and characteristics of the process of BCS-regime formation in a spiral nonrelativistic electron stream with additional beam deceleration.

BCS studies were conducted by the example of a vircator with an electron source as a magnetron–injection gun (MIG) [12]. The choice of an MIG system was predetermined by its ability to apply a significant external magnetic field to form a BCS. In addition, the MIG has a high perveance, which makes it an efficient electron source for optimizing the work of a generator with electronic feedback [12, 13].

The MIG processes were modeled numerically with the help of a previously designed 2.5D mathematical model based on a self-congruent system of motion equations and Poisson's equation for finding the self-congruent field of a spatial charge [14]. The dynamics of an electron stream was modeled by the large-particle method (PIC method).

Figure 1a shows schematically the geometry of the system studied by the numerical model. An axisymmetrical model of the system under study was considered. The upper half plane of the section plane (r, z) of the drift space between cathode *1* and anode *2* was modeled in the paper. The shaded section on cathode *1* corresponds to strip-emitting MIG *3*, on which electron stream *4* is formed. The drift chamber is split into two parts, and the deceleration potential, which is smaller than anode potential $\varphi_r < \varphi_a$, is applied to the chamber's right part *5*.
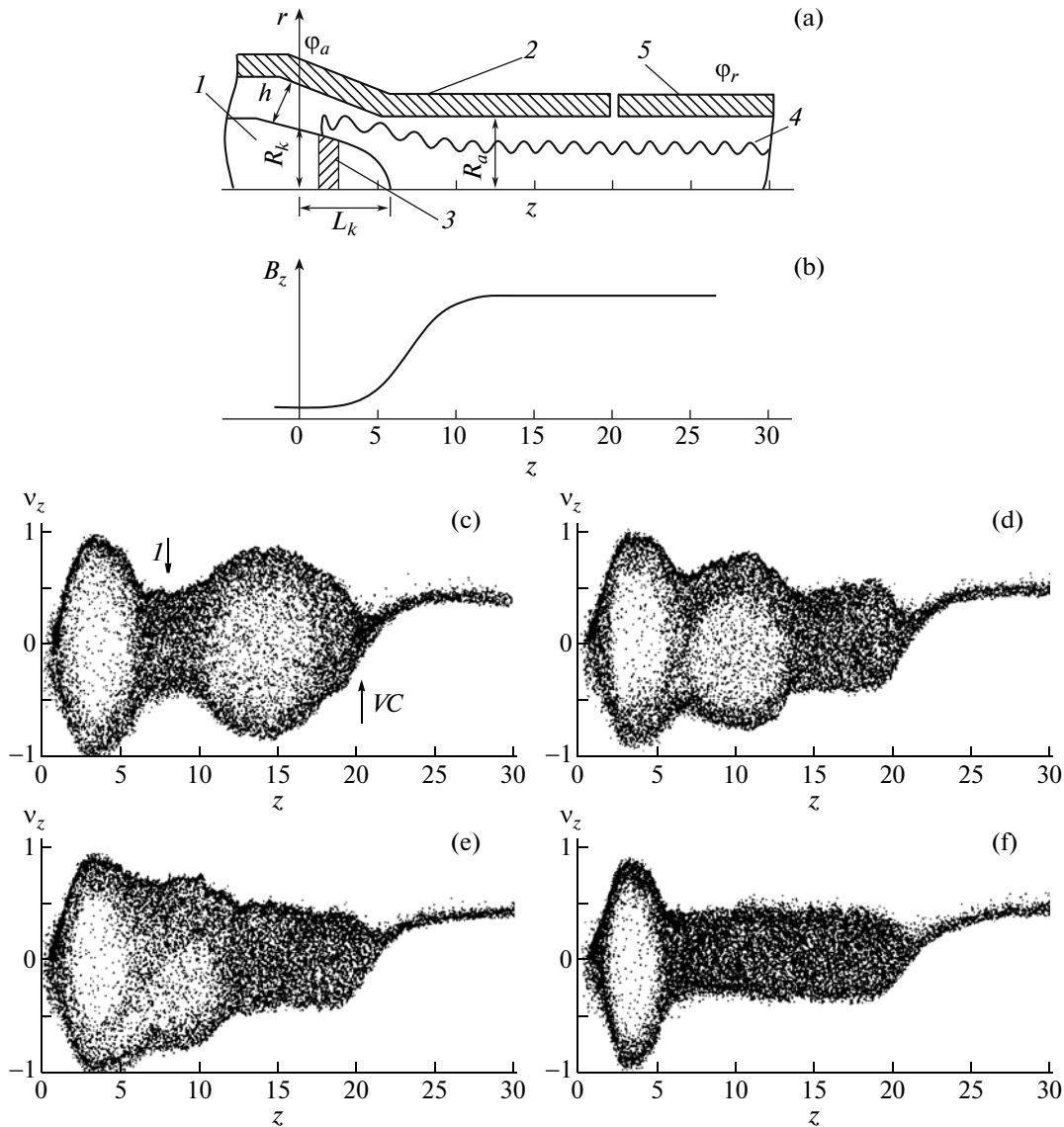
Fig. 1. (a) Diagram of the magnetron–injection gun: (*1*) cathode, (*2*) acceleration electrode with potential φ_a, (*3*) emitting strip, (*4*) electron stream, (*5*) decelerating electrode with potential φ_r, $L_k = 17.8$ mm, $R_k = 7.4$ mm, $h = 3$ mm, and $R_a = 8.4$ mm. The dimensions given in the figure were normalized by h; the scales of the horizontal and vertical axes mismatch. (b) The distribution of the longitudinal component of magnetic field B_z in the drift space; (c), (d), (e), and (f) phase portraits of the beam in coordinates (z, v_z) for various time points $(t_1 < t_2 < t_3 < t_4)$. The arrows (c) mark the area of particle deceleration owing to the magnetic trap (arrow *1*) and the VC area (arrow *VC*).

During MIG modeling, the Maxwellian law of distribution of the full thermal velocities of ejected electrons was taken into account. The MIG magnetic field in the area of moving electrons meets the paraxiality condition (Fig. 1b); in addition, the field configuration in the gun cathode area represents a magnetic trap (in the area of cathode *1*, longitudinal value B_z of the magnetic field is smaller than in the drift tube area).

Gun parameters for numerical modeling were chosen in line with [15], which investigated the complex dynamics of a MIG-formed beam. In the numerical experiment, the density of the beam current was equivalent to $j_0 = 4.7$ A/cm^2 at an accelerating voltage of 2000 V with guiding magnetic field $B_k = 300$ Gs (in the cathode area), and $B_0 = 800$ Gs in the drift space. The following geometrical parameters of the gun were chosen: MIG cathode length $L_k = 17.8$ mm (see the legend to Fig. 1a), cathode radius $R_k = 7.4$ mm, distance between the cathode and the anode $h = 3$ mm, drift tube radius $R_a = 8.4$ mm, and total length of the gun and the drift space $L = 90$ mm (not shown in Fig. 1a). Hereinafter, including the figures, all values are given in normalized units; the geometric dimensions were normalized by h.

Let us discuss the results of modeling this system. The investigation has shown that the model under consideration can establish a BCS in a certain area of control parameters. Figures 1c−1f show the phase portraits of an electron beam in dimensionless coordinates (z, v_z) for various time points ($t_1 < t_2 < t_3 < t_4$). The time points were chosen to demonstrate various stages of BCS formation in a spiral beam.

In the range of values of longitudinal coordinate z, which corresponds to gap 5 in the drift space, a VC is formed (arrow VC in Fig. 1c) due to the introduction of additional deceleration. In this system, following the classification in [3], the VC may be classed as a reflex VC. Moreover, since the system has a magnetic trap in the cathode area and a wide spread of thermal velocities in the electron stream, which is typical of an MIG (and which accelerates when electrons move along the drift space [12]), here we have signs of a magnetic and thermal VC [3]. Charged particles are reflected in the VC area, resulting in the establishment of a two-stream state in the MIG cathode−VC area.

As we see in Fig. 1c, in the beginning of BCS formation, we can observe spatial-charge concentrations near the magnetic trap, where electrons experience additional deceleration owing to the field effect of the magnetic trap (arrow 1 in the figure), as well as near the deceleration electrode in the VC area (arrow VC). Before the point of full BCS establishment, spatial-charge concentrations can appear and disappear in time, replacing alternately one another or appearing simultaneously.

At the next stage in time, the higher density area of the spatial charge near the decelerating electrode begins to extend in space from the VC toward the MIG cathode (Figs. 1d and 1e). Simultaneously, the charge density in the area of the magnetic trap decreases slightly and the charged particles either deposit on the electrodes (the cathode and the anode) or leave for the drift space area. As a result, an electron cloud consisting of low-velocity particles is formed in a certain extended area of the beam and an even density distribution of the spatial charge, which corresponds to the BCS, is established in this cloud (Fig. 1f).

As was said above, the BCS, in fact, represents a distributed VC. The phase portrait that corresponds to the compressed state (Fig. 1f) shows that the axial velocity of electrons in the beam in the area of this extended VC does not exceed dimensionless value $v_z \approx$ 0.5. Velocity is normalized by characteristic value v_0—the axial velocity of near-anode electrons that left the cathode with a zero velocity and accelerated in the anode field with potential φ_a. Figure 1f also shows that no BCS is observable in the cathode area; axial velocities v_z of the beam electrons are much higher here than in the BCS area. This is due to the acceleration of the beam electrons in the anode field near the cathode. In addition, the absolute value of their longitudinal velocity will depend on the spin phase in the magnetic field. The axial velocity of the beam also increases (to

values of $v_z \approx 1$) owing to the exit from the magnetic trap. All this hinders efficient BCS establishment in this area.

Note that the BCS establishment process in a spiral beam with deceleration is reminiscent of a similar process in a relativistic beam in the composite drift tube, where a wave of switching the beam's two-stream state to a BCS was revealed [9]. In particular, the wavefront of this switching can be used to accelerate ions. In the case of a spiral beam in a system with deceleration, this process is not expressed vividly and can be adjusted significantly depending on the values of control parameters, namely, the beam current and deceleration potential φ_r.

Let us note some other characteristics of BCS establishment and dynamics in a spiral beam with deceleration. Figure 2 shows time dependences of the potential of the drift-space point on time for two values of deceleration potential $\Delta\varphi = \varphi_a - \varphi_r$. Analysis of space potential dynamics in the beam area allows a detailed study of the process of accumulating and discharging the spatial charge in the system. For the case given in Fig. 2, the point where the potential was measured is located on the right end of the drift space, $z =$ 25, at the beam boundary (i.e., outside of the limits of the compressed-state area).

Numeral 1 in Fig. 2 designates dependence $\varphi(t)$ at $\Delta\varphi = 1.3$, at which a BCS has not been formed fully. In this case, the oscillations of the potential correspond to well-marked noise fluctuations, which depend on the complex VC dynamics in a beam with a large spread of electron velocities [16]. Then, as deceleration increases, the system forms a well-developed BCS. This state is characterized, first, by a significant increase in the accumulated charge. This is manifested by a decrease in the average potential value near which oscillations occur (dependence 2 in Fig. 2, constructed at $\Delta\varphi = 1.5$). Second, powerful low-frequency oscillations of the potential start to manifest themselves more vividly in temporal dependence $\varphi(t)$. Studies show that, in this case, intense longitudinal oscillations of the spatial charge develop in the area between the VC and the MIG cathode in the electron cloud that corresponds to the BCS. In addition, compact bunches of electrons leave the compressed state area with a certain degree of periodicity.

We may assume that the appearance of such longitudinal charge dynamics, as the beam density increases in the BCS mode, is characteristic of the considered case of a system with deceleration. We recall that a BCS in a relativistic case is formed in the extended drift area, where the limit vacuum current of VC formation is not exceeded [3, 6]. The stud for BCS origin is a VC forming in the next area of the drift space, where the limit vacuum current is lower than in the BCS formation space. However, in the relativistic case, the attempt to increase significantly the charge density of the beam in a BCS to produce such axial oscillations runs into the problem of a secondary VC
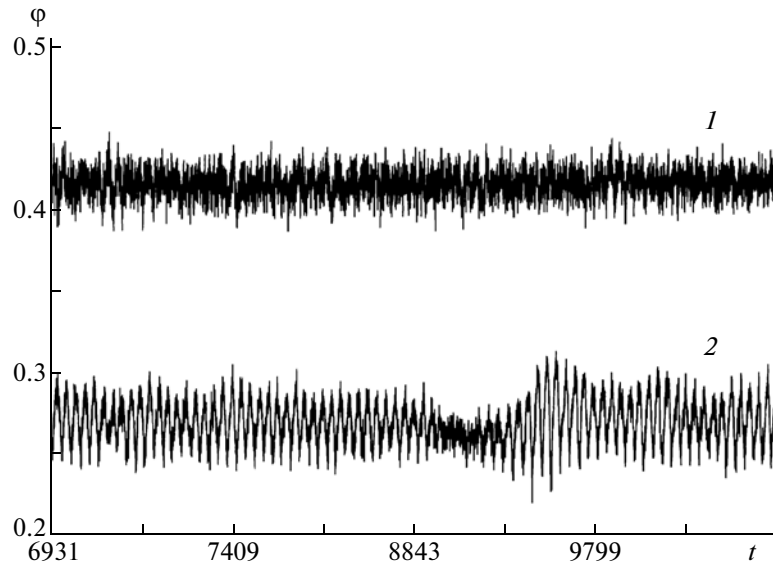
Fig. 2. The dependence of the drift-space potential on time (in normalized units) for two values of the decelerating differentials of the potentials: (*1*) $\Delta\varphi = 1.3$ and (*2*) $\Delta\varphi = 1.5$.

emerging in the BCS area. At the same time, such a problem does not arise in a system with deceleration, since, in this case, the limit vacuum current can be substantially larger than the current of an electron beam.

Thus, this paper describes the results of numerical modeling of establishing a compressed state in an intense spiral electron stream with additional deceleration. This article describes the mechanism of BCS establishment in a nonrelativistic system, showing that a nonrelativistic system with deceleration is characterized by the emergence of longitudinal dynamics of a spatial charge in a compressed stream state, which is probably not typical of relativistic beams.

REFERENCES

1. A. A. Rukhadze, S. D. Stolbetsov, and V. P. Tarakanov, Radiotekh. Elektron. **37**, 385 (1992).

2. A. E. Dubinov and V. D. Selemir, J. Commun. Technol. Electron. **47**, 575 (2002).

3. A. E. Dubinov, I. A. Efimova, I. Yu. Kornilova, S. K. Saikov, V. D. Selemir, and V. P. Tarakanov, Phys. Particles Nuclei **35**, 251 (2004).

4. J. Benford, J. A. Swegle, and E. Schamiloglu, *High Power Microwaves*, 2nd ed. (Taylor and Francis, New York, 2007).

5. A. M. Ignatov and V. P. Tarakanov, Phys. Plasmas **1**, 741 (1994).

6. A. E. Dubinov, Tech. Phys. Lett. **23**, 870 (1997).

7. A. E. Dubinov, I. V. Makarov, S. A. Sadovoi, S. K. Saikov, and V. P. Tarakanov, Tech. Phys. Lett. **37**, 230 (2011).

8. V. N. Barabanov, A. E. Dubinov, M. V. Loiko, S. K. Saikov, V. D. Selemir, and V. P. Tarakanov, Plasma Phys. Rep. **38**, 169 (2012).

9. A. E. Dubinov, I. Yu. Kornilova, and V. D. Selemir, Phys. Usp. **172**, 1225 (2002).

10. Yu. A. Kalinin, A. A. Koronovskii, A. E. Khramov, E. N. Egorov, and R. A. Filatov, Plasma Phys. Rep. **31**, 1009 (2005).

11. E. N. Egorov, Yu. A. Kalinin, A. A. Koronovskii, D. I. Trubetskov, and A. E. Khramov, Radiophys. Quantum Electron. **49**, 760 (2006).

12. E. N. Egorov and A. E. Khramov, Tech. Phys. Lett. **36** (2010).

13. E. N. Egorov and A. E. Khramov, Izv. Vyssh. Ucheb. Zaved.: Probl. Nelin. Dinam. **19** (4), 40 (2011).

14. A. E. Khramov, S. A. Kurkin, E. N. Egorov, A. A. Koronovskii, and R. A. Filatov, Mat. Model. **23** (1), 3 (2011).

15. Yu. A. Kalinin, V. N. Kozhevnikov, A. G. Lazerson, G. I. Aleksandrov, and E. E. Zhelezovskii, Tech. Phys. **45**, 896 (2000).

16. Yu. A. Kalinin and A. E. Khramov, Tech. Phys. **51**, 558 (2006).

Translated by B. Alekseev